**Phototransformation of Vanillin in Artificial Snow by Direct Photolysis and Mediated by Nitrite**

(Article begins on next page)

03 May 2024

# Supporting Information

**Phototransformation of vanillin in artificial snow by direct photolysis and mediated by nitrite**
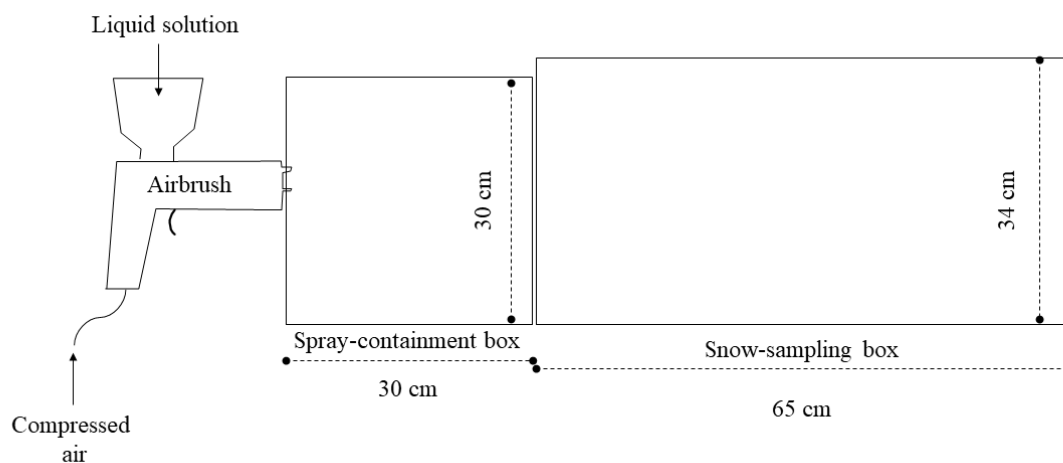
Luca Carena,* Beatrice Zoppi, Fabrizio Sordello, Debora Fabbri, Marco Minella, Claudio Minero*

*Department of Chemistry, University of Torino, via P. Giuria 5, 10125 – Torino (Italy)*

* Address correspondence to either author: *luca.carena@unito.it* (LC), *claudio.minero@unito.it* (CM)

# Contents:

**(a)**



**(b)**



**(c)**

**Fig.SI-1. (a)** Schematic showing the lab set-up used for artificial-snow preparation inside the cold room at 243 K. **(b)** Picture of a typical snow sample prepared for irradiation experiments. **(c)** Snow samples irradiated at 243 K under the adopted LED set-up emitting in the UVA light spectrum.

**Text SI-1. Determination of the specific surface area of artificial snow.**

The high-performance adsorption analyzer ASAP 2020 Plus (Micrometrics) was used for measuring the specific surface area (SSA) of artificial snow. The adsorption isotherm of Kr on artificial snow (sample of ~ 152 g) was measured at liquid nitrogen temperature (77 K). Although snow SSA is usually measured by $CH_4$ adsorption at 77 K,[1–3] in this work we adopted Kr for its very low saturation vapor pressure ($P_0$) at that temperature.[4] Furthermore, Kr has chemical-physical features that would make it as suitable as $CH_4$ for this kind of measurements. The analytical protocol described previously by Legagneux et al.[1] was followed for snow-SSA determination. Nine points of the B.E.T. isotherm were recorded between $P/P_0 = 0.07$ and $P/P_0 = 0.22$ (Fig.SI-2), of which interpolation allowed to assess the snow SSA $= 369$ cm$^2$ g$^{-1}$.



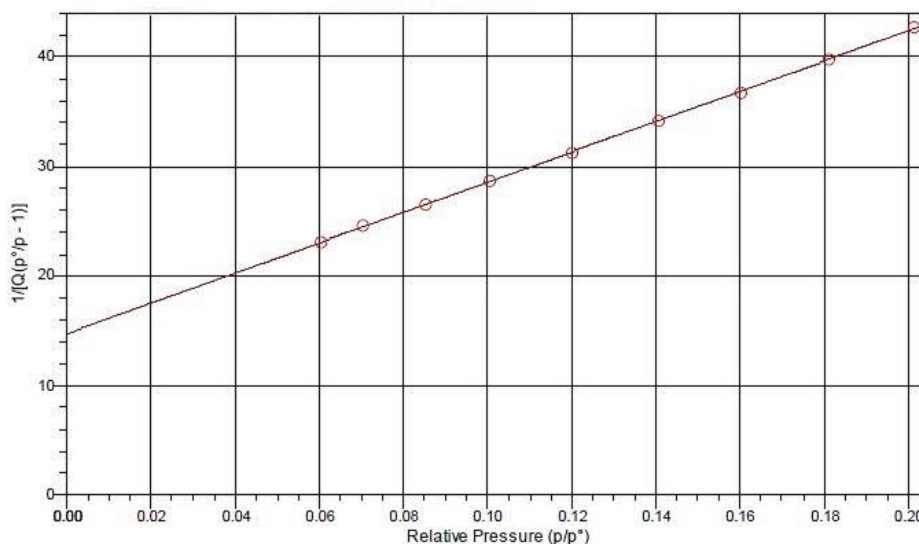**Fig.SI-2.** B.E.T surface area plot recorded for an artificial snow sample.

**Text SI-2. HPLC-DAD and HPLC-MS/MS analysis**

Irradiated samples of snow and liquid water were analyzed for quantitation of residual VN by means of high-performance liquid chromatography coupled with diode array detection (HPLC-DAD). The instrument was a VWR-Hitachi Chromaster equipped with 5260 autosampler (60 µL injection volume),

5160 quaternary pump and 5430 DAD detector. The column was a Merck LiChroCART RP-18 cartridge (125 mm × 4 mm × 5 µm), and isocratic elution was carried out with a 70:30 mixture of (A) acidified water (H$_3$PO$_4$, pH 2.8) and (B) methanol at eluent flow rate 1 mL min$^{-1}$. The VN retention time was 5.5 min, while the detection wavelength of 230 nm. For vanillic acid and acetovanillone quantification, the isocratic elution 65:35 = A:B was used (flow rate = 1 mL min$^{-1}$), showing a retention time of 4.8 min for vanillic acid and 5.3 min for acetovanillone (the detection wavelengths were 260 and 230 nm, respectively).

For 2NB quantification in chemical actinometry, the elution (flow rate = 1 mL min$^{-1}$) was carried out with a 62:38 mixture of eluent A and B, respectively. 50 µL was the injection volume. The 2NB retention time was 5.6 min, while the detection wavelength of 223 nm.

Under some irradiation conditions (see the main manuscript), nitrite was quantified as well. Pre-column derivatization with 2,4-dinitrophenylhydrazine (2,4DNPH) was used following the method of Kieber and Seaton.[5] The derivatization of 2,4DNPH in acidic solution produces the corresponding azide (2,4-dinitrophenylazide, 2,4DNPA), which can be detected by HPLC-DAD. Operationally, 50 µL of the derivatizing agent (composed of ultrapure water + HCl + CH$_3$CN, previously purified by extraction with CCl$_4$) was added to 2 mL of irradiated sample and let it react for 10 min under magnetic stirring. The derivatized sample was then analyzed by HPLC-DAD, eluting with a 50:50 mixture of A and B at 1 mL min$^{-1}$ flow rate. The retention time of 2,4DNPA was 3.5 min and the quantification wavelength was 307 nm. Because 2,4DNPH can react with aromatic carbonyls forming 2,4-dinitrophenylhydrazones, and nitrite can react with vanillin under acidic conditions, the standard solutions of nitrite used for calibration contained 5 µmol L$^{-1}$ VN. The method predicted well the concentration of nitrite in snow samples at time zero (i.e., before irradiation).

A UFLC-SHIMADZU combined with 3200 QTRAP LC/MS/MS system from SCIEX (Framingham, MA, USA) was used for identification of the intermediate photoproducts. Chromatographic separation

was performed with a column Synergi 4µm Fusion RP (Phenomenex, 50 x 2 mm) and a mobile phase consisting of a mixture of ammonium acetate (5 mmol $L^{-1}$, eluent A) and acetonitrile (eluent B) with a flow rate = 0.4 mL $min^{-1}$. The gradient elution was as follows: 0.1–15 min from 5% to 100% B, 15-17 min 100% B, 17-17.5 min from100 to 5 % B, 17.5-20 min 5% B. The column oven temperature was set to 40 °C and the injection volume was 10 µL. Electrospray ionization (ESI) was used in negative ion mode and the source parameters were as follows: ionspray voltage = -3500 eV; ion source temperature = 300 °C; curtain gas = 25 psi; declustering potential = -45 V; ion spray gas = 45 psi. For issues of instrumental sensitivity, analysis were firstly run in full mass mode (mass range 50–400 $m/z$) and then in single ion monitoring (SIM) mode for the following [M-H]$^-$ ($m/z$) ions: 137, 151 (VN), 167, 168, 183, 196, 301 and 318 to confirm their presence. The choice for these ions was based on photoproducts previously identified for VN direct photolysis, reaction with HO$^{\bullet}$ radicals and its nitrite-photosensitized transformation in liquid water under different irradiation conditions.[6–8] For tentative identification, HPLC-MS$^2$ analysis were then carried out with a collision energy = 25 eV and all MS$^2$ spectra were collected by enhanced product ions (EPI) mode.
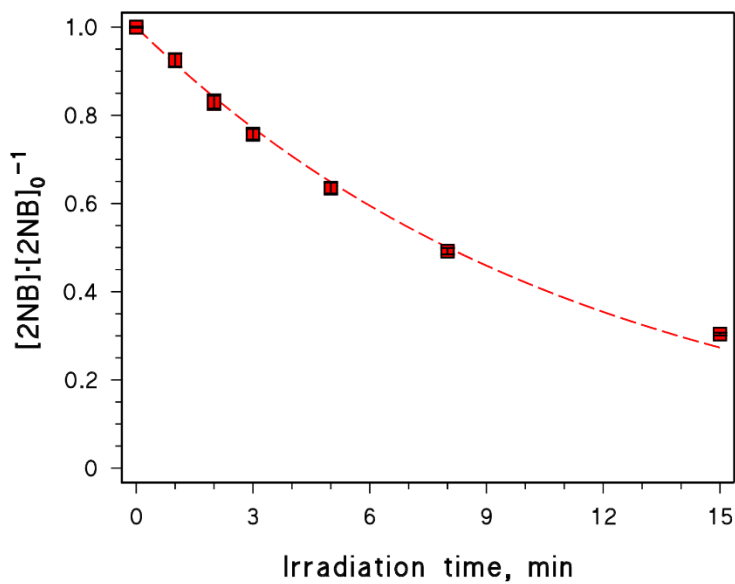
**Fig.SI-3.** Observed photodegradation of 2NB in artificial snow at 243 K. Error bars represent the standard deviation of duplicate runs, while the dotted red line is the fit curve of experimental data. In particular, only data for which $[2NB] \, [2NB]_0^{-1} \geq 0.6$ were used for the computation of the first-order rate constant $k'_{2NB}$, to minimize the light-absorption competition due to the formation of 2-nitrosobenzoic acid from the photoisomerization of 2NB.[9,10]
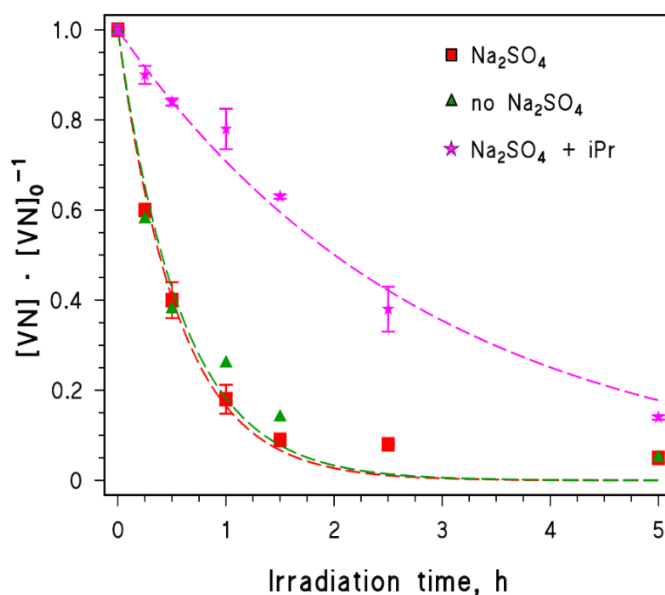


**Fig.SI-4.** Profiles of VN (5 µmol L$^{-1}$) concentration, as a function of the irradiation time, in liquid water at room temperature in the presence of Na$_2$SO$_4$ (65 µmol L$^{-1}$), without Na$_2$SO$_4$ and in the presence of 500 µmol L$^{-1}$ iPr + 65 µmol L$^{-1}$ Na$_2$SO$_4$. Note that in the latter case the total solute concentration was 700 µmol L$^{-1}$. The dotted lines are the fit curves of experimental data, whereas the error bars are the standard deviation of duplicate runs.

**Fig.SI-5**. Profiles of nitrite and vanillin (49 and 5 µmol L⁻¹ as initial concentrations, respectively) observed in artificial snow (243 K) with added 31.6 µmol L⁻¹ Na₂SO₄, as a function of time. The loss of the compounds measured after 5 h of UVA irradiation is reported as $\Delta[S]_{5h}$.
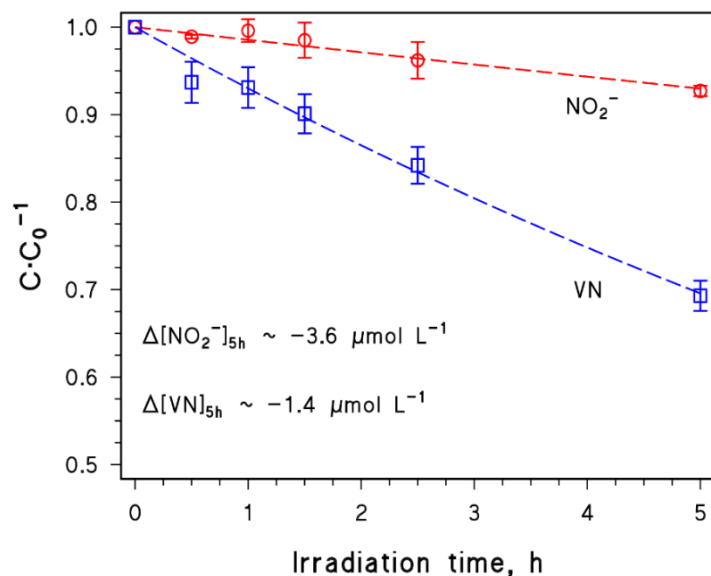
**Text SI-3. Assessment of the photon flux densities absorbed by vanillin and nitrite in snow samples.**

Both VN and nitrite in snow samples absorb the UVA light emitted by the adopted LED lamp. The photon flux density absorbed by one species ($P_a$, Ein L⁻¹ s⁻¹) can be assessed by taking into account the competition between VN and $NO_2^-$ for light absorption.

$$P_a(\text{VN}) = \sum_\lambda p^0(\lambda) \frac{A_{\lambda, \text{VN}}}{A_{\lambda, \text{VN}} + A_{\lambda, NO_2^-}} \left[1 - 10^{-\left(A_{\lambda, \text{VN}} + A_{\lambda, NO_2^-}\right)}\right] \Delta\lambda \qquad \text{(Eq. SI-1)}$$

$$P_a(NO_2^-) = \sum_\lambda p^0(\lambda) \frac{A_{\lambda, NO_2^-}}{A_{\lambda, \text{VN}} + A_{\lambda, NO_2^-}} \left[1 - 10^{-\left(A_{\lambda, \text{VN}} + A_{\lambda, NO_2^-}\right)}\right] \Delta\lambda \qquad \text{(Eq. SI-2)}$$

$p^0(\lambda)$ is the spectral photon flux density of the lamp passing through the snow samples (Ein s⁻¹ L⁻¹ nm⁻¹), and determined by chemical actinometry. $A_{\lambda, \text{VN}}$ and $A_{\lambda, NO_2^-}$ are, respectively, the Lambert-Beer absorbance of VN and nitrite in snow samples, determined as $A_{\lambda, \text{VN}} = \varepsilon_{\lambda, \text{VN}} \, l \, [\text{VN}]$ and $A_{\lambda, NO_2^-} =$

$\varepsilon_{\lambda, NO_2^-} \, l \, [NO_2^-]$, where $\varepsilon_{\lambda, VN}$ and $\varepsilon_{\lambda, NO_2^-}$ are the molar absorption coefficient (L mol$^{-1}$ cm$^{-1}$) of VN and

nitrite, while $l = 1.8$ cm is the optical path of the snow sample. Note that the molar absorption coefficient

of phenols has been found to undergo bathochromic shifts of few nm in the UV range when present on

the surface of ice grains.[11] Here, we used $\varepsilon_{\lambda, VN}$ determined in liquid water because that in snow is

unfortunately unknown. Therefore, if a red shift is operational also in the case of VN, $P_a(VN)$ determined

with Eq. SI-1 would be slightly underestimated. Instead, a previous study showed that $\varepsilon_{\lambda, NO_2^-}$ does not

significantly vary with temperature.[12]

The total absorbed photon flux density by the snow sample will be:

$$P_a(\text{tot}) = \sum_{\lambda} p^0(\lambda) \left[ 1 - 10^{-\left( A_{\lambda, VN} + A_{\lambda, NO_2^-} \right)} \right] \Delta\lambda \qquad \text{(Eq. SI-3)}$$

The fraction of UVA light absorbed by VN can be calculated as $P_a(VN) \, [P_a(\text{tot})]^{-1}$, while that by nitrite

will be $P_a(NO_2^-) \, [P_a(\text{tot})]^{-1}$. Fig. SI-6 shows that the main light-absorbing species in our snow samples

is VN, regardless of nitrite concentration.



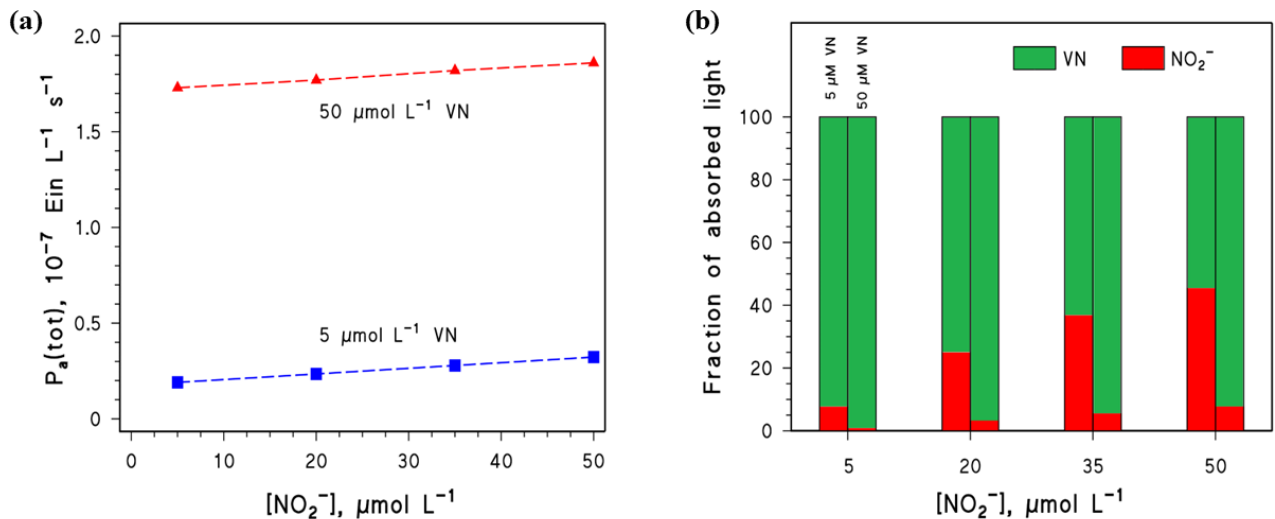**Fig.SI-6. (a)** Total photon flux density absorbed by snow samples containing VN and nitrite, as computed with Eq. SI-3. **(b)** Fractions of light absorbed by VN and nitrite in the irradiated snow samples, as functions of nitrite concentration.

**Text SI-4. Photodegradation pathways of vanillin in snow samples.**

As described in the main manuscript, the most likely reactive species that trigger VN photodegradation in snow with added nitrite under UVA light are $^{\bullet}NO_2$, HOONO and $HO^{\bullet}$, as well as direct photolysis. For simplicity, hereinafter $^{\bullet}NO_2$ + HOONO = RNS (Reactive Nitrogen Species). The total photodegradation rate of VN can be written as sum of the rates of each transformation pathway, as $R_{VN} = R_{VN,d.p.} + R_{VN,HO^{\bullet}} + R_{VN,RNS}$. By dividing for the initial VN concentration and normalizing for the photon flux $P^0$, one gets the previous equation in terms of rate coefficients: $k_{VN}^{\prime,n} = k_{VN,d.p.}^{\prime,n} + k_{VN,HO^{\bullet}}^{\prime,n} + k_{VN,RNS}^{\prime,n}$. Note that $k_{VN}^{\prime,n}$ was assessed with the irradiation experiments.

*Direct photolysis.* It is possible to compute $k_{VN,d.p.}^{\prime,n}$ in the presence of nitrite by correction of the $k_{VN,d.p.}^{\prime,n}$ value obtained in absence of nitrite (i.e., experiments of VN direct photolysis; here, $k_{VN,d.p.}^{\prime,n,0}$) for the light-absorption competition between VN and nitrite. Indeed, by absorbing UVA light, nitrite can limit VN direct photolysis.

$$k_{VN,d.p.}^{\prime,n} = k_{VN,d.p.}^{\prime,n,0} \frac{\sum_{\lambda} p^0(\lambda) \frac{A_{\lambda, VN}}{A_{\lambda, VN} + A_{\lambda,NO_2^-}}\left[1 - 10^{-\left(A_{\lambda, VN}+A_{\lambda,NO_2^-}\right)}\right]\Delta\lambda}{\sum_{\lambda} p^0(\lambda)[1 - 10^{-A_{\lambda, VN}}]\Delta\lambda} \qquad \text{(Eq. SI-4)}$$

It was $k_{VN,d.p.}^{\prime,n,0} = 0.43 \pm 0.03$ L Ein$^{-1}$ for 5 µmol L$^{-1}$ as initial VN concentration, while no obvious photodegradation was observed for 50 µmol L$^{-1}$ VN after 24 h (see Fig.2 of the main manuscript).

*Reaction with HO$^{\bullet}$ radical.* $k_{VN,HO^{\bullet}}^{\prime,n}$ can be written as $= k_{VN,HO^{\bullet}} [HO^{\bullet}](P^0)^{-1}$, where $k_{VN,HO^{\bullet}}$ is the bimolecular rate constant of the reaction between VN and HO$^{\bullet}$. $k_{VN,HO^{\bullet}} = 4 \cdot 10^8$ L mol$^{-1}$ s$^{-1}$ has been determined in liquid water,[6] and its value in snow at 243 K is unfortunately unknown. $[HO^{\bullet}]$ is the concentration of hydroxyl radicals in the irradiated snow samples and can be assessed by means of the steady-state approximation, considering its photoproduction and loss by reaction with VN and nitrite.

$$[HO^\bullet] = \frac{R_{f,HO^\bullet}}{k_{VN,HO^\bullet}\,[VN] + k_{NO_2^-,HO^\bullet}\,[NO_2^-]} \qquad\qquad \text{(Eq. SI-5)}$$

$k_{NO_2^-,HO^\bullet}$ is the second-order rate constant of nitrite oxidation by $HO^\bullet$, and its value in liquid water is $1\cdot10^{10}$ L mol$^{-1}$ s$^{-1}$ (in snow at 243 K, it is unfortunately unknown).[13] $R_{f,HO^\bullet}$ is the photoproduction rate of $HO^\bullet$ in snow samples, and can be determined as $R_{f,HO^\bullet} = 2.303\,[NO_2^-]\,l\sum_\lambda \phi_{NO_2^-,HO^\bullet}(\lambda)\,p^0(\lambda)\,\varepsilon_{\lambda,\,NO_2^-}\,\Delta\lambda$ for a low-absorbing medium (as in our case), where $\phi_{NO_2^-,HO^\bullet}(\lambda)$ is the quantum yield of nitrite photolysis to yield $HO^\bullet + {}^\bullet NO$. A previous work has determined its dependence on both wavelength (nm) and temperature (K) in ice, as follows:[12]

$$\phi_{NO_2^-,HO^\bullet}(\lambda) = \left[0.0204 + \frac{0.0506}{1 + e^{\frac{\lambda - 332}{11.2}}}\right] e^{\left[\frac{20.5\,\lambda + 7553}{8.314}\left(\frac{1}{295} - \frac{1}{T}\right)\right]} \qquad\qquad \text{(Eq. SI-6)}$$

Fig. SI-7 shows the spectral photoproduction rate of $HO^\bullet$, $R_{f,HO^\bullet}(\lambda) = 2.303\,[NO_2^-]\,l\,\phi_{NO_2^-,HO^\bullet}(\lambda)\,p^0(\lambda)\,\varepsilon_{\lambda,\,NO_2^-}$, as computed for our snow samples at different nitrite concentrations.
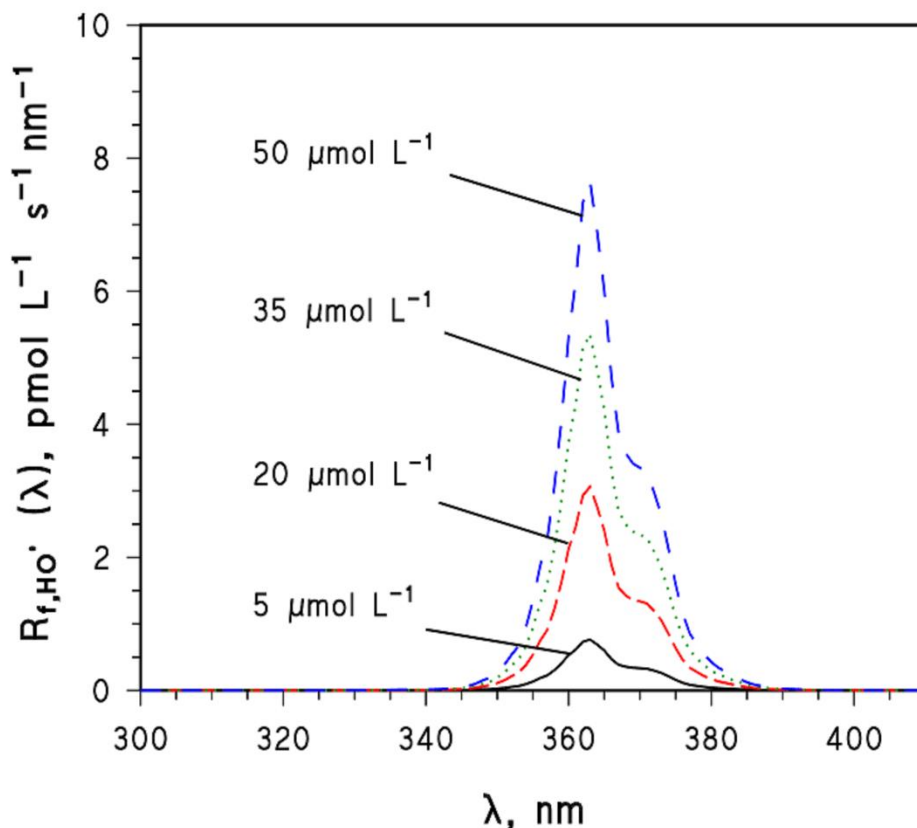
**Fig.SI-7**. Spectral photoproduction rate of hydroxyl radicals in the irradiated snow samples, at different concentrations of nitrite. Note that the total rate of HO• formation is the integral of each curve.

Note that nitrite was here considered to be the main photosensitizer of HO•, while HONO was not taken into account. The $pK_a$ of HONO is ~ 2.8 and it is more efficient than nitrite as HO• photosensitizer.[14] Therefore, one can expect a higher photoproduction rate of HO• in the QLL for pH < 2, but we do not know the actual pH of the QLL in snow samples. However, the use of $Na_2SO_4$ to fix the total solute concentration would have made QLL acidic because of the Workman-Reynolds effect,[15] but we did not observe significant loss of nitrite during snow preparation due to nitrite protonation in the QLL and subsequent HONO volatilization.[14] Therefore, we can infer that the pH of the QLL was acidic but > 3, condition at which nitrite is the main species of added N(III).

*Reaction with RNS.* Finally, $k'^{,n}_{VN,RNS}$ was computed as $= k'^{,n}_{VN} - k'^{,n}_{VN,d.p.} - k'^{,n}_{VN,HO•}$.

The role played by each pathway in the overall VN photodegradation was assessed as the ratio between the computed rate coefficient for that pathway ($k'^{,n}_{VN,d.p.}$, $k'^{,n}_{VN,HO\bullet}$ or $k'^{,n}_{VN,RNS}$) and the observed rate coefficient of VN photodegradation ($k'^{,n}_{VN}$).

**Text SI-5. $k'^{,n}_{VN,RNS}$ and the steady-state concentration of $^\bullet NO_2$ and HOONO in artificial snow.**

At constant 50 µmol $L^{-1}$ $NO_2^-$, reactions with RNS were the main VN degradation pathways regardless of [VN], as shown in Table 1 of the main manuscript. Therefore, one has that $k'^{,n}_{VN} = k'^{,n}_{VN,d.p.} + k'^{,n}_{VN,HO\bullet} + k'^{,n}_{VN,RNS} \cong k'^{,n}_{VN,RNS}$. As done for $k'^{,n}_{VN,HO\bullet}$ above, $k'^{,n}_{VN,RNS}$ can be written as $= \left(k^{app}_{VN,NO_2}[^\bullet NO_2] + k^{app}_{VN,HOONO}[HOONO]\right)(P^0)^{-1}$, where $k^{app}_{VN,NO_2}$ and $k^{app}_{VN,HOONO}$ are the apparent bimolecular rate constants of the VN reactions with $^\bullet NO_2$ and HOONO, respectively. The concentrations of the latter can be derived by considering the steady-state approximation and the reactions reported in Scheme SI-1. In particular, one has:

$$[^\bullet NO_2] = \frac{R_{f,NO_2}}{k'_{loss,NO_2} + k_{VN,NO_2}[VN] + k_{VN^{\bullet+},NO_2}[VN^{\bullet+}]} \qquad \text{(Eq.SI-7)}$$

$$[HOONO] = \frac{k_{NO,HO_2^\bullet}[^\bullet NO][HO_2^\bullet]}{k'_{iso} + k_{VN,HOONO}[VN]} \qquad \text{(Eq.SI-8)}$$

$R_{f,NO_2}$ is the formation rate of $^\bullet NO_2$ and can be expressed as per Eq.SI-9.

$$R_{f,NO_2} = k_{NO_2^-,HO\bullet}[NO_2^-][HO^\bullet] + k'_{O_2,^\bullet NO}[^\bullet NO] + k_{NO_2^-,^3VN^*}[NO_2^-][^3VN^*]$$

$$+ k_{NO_2^-,VN^{\bullet+}}[NO_2^-][VN^{\bullet+}] \qquad \text{(Eq.SI-9)}$$

By substituting Eq.SI-5 and considering that $k_{VN,HO\bullet}[VN] \ll k_{NO_2^-,HO\bullet}[NO_2^-]$ for 50 µmol $L^{-1}$ $NO_2^-$, one has:

$$R_{f,NO_2} = R_{f,HO\bullet} + k'_{O_2,^\bullet NO}[^\bullet NO] + [NO_2^-]\left(k_{NO_2^-,^3VN^*}[^3VN^*] + k_{NO_2^-,VN^{\bullet+}}[VN^{\bullet+}]\right) \qquad \text{(Eq.SI-10)}$$

The steady-state concentration of $^\bullet NO_2$ will read as follows:

$$[^\bullet NO_2] = \frac{R_{f,HO^\bullet} + k'_{O_2,^\bullet NO}[^\bullet NO] + [NO_2^-]\left(k_{NO_2^-,^3VN^*}[^3VN^*] + k_{NO_2^-,VN^{\bullet+}}[VN^{\bullet+}]\right)}{k'_{loss,NO_2} + k_{VN,NO_2}[VN] + k_{VN^{\bullet+},NO_2}[VN^{\bullet+}]} \qquad \text{(Eq.SI-11)}$$

Note that $[^\bullet NO] = R_{f,HO^\bullet}\left(k'_{loss,NO} + k'_{O_2,^\bullet NO} + k_{NO,HO_2^\bullet}[HO_2^\bullet]\right)^{-1}$ under the steady-state approximation and $R_{f,HO^\bullet} = 2.303\,[NO_2^-]\,l\sum_\lambda \phi_{NO_2^-,HO^\bullet}(\lambda)\,p^0(\lambda)\,\varepsilon_{\lambda,\,NO_2^-}\,\Delta\lambda = [NO_2^-]k'_{f,HO^\bullet}$ as described in the previous section.

$$[^\bullet NO_2] = [NO_2^-]\frac{k'_{f,HO^\bullet}(1+\tau) + \left(k_{NO_2^-,^3VN^*}[^3VN^*] + k_{NO_2^-,VN^{\bullet+}}[VN^{\bullet+}]\right)}{k'_{loss,NO_2} + k_{VN,NO_2}[VN] + k_{VN^{\bullet+},NO_2}[VN^{\bullet+}]} \qquad \text{(Eq.SI-12)}$$

$$[HOONO] = [NO_2^-]\frac{k'_{f,HO^\bullet}\,\tau'}{k'_{iso} + k_{VN,HOONO}[VN]} \qquad \text{(Eq.SI-13)}$$

Where $\tau = k'_{O_2,^\bullet NO}\left(k'_{loss,NO} + k'_{O_2,^\bullet NO} + k_{NO,HO_2^\bullet}[HO_2^\bullet]\right)^{-1}$ and $\tau' = k_{NO,HO_2^\bullet}[HO_2^\bullet]\left(k'_{loss,NO} + k'_{O_2,^\bullet NO} + k_{NO,HO_2^\bullet}[HO_2^\bullet]\right)^{-1}$.

Finally, when RNS reactions account for the main VN photodegradation in snow samples (i.e., $k'^{,n}_{VN} \cong k'^{,n}_{VN,RNS}$), since $k'^{,n}_{VN,RNS} = \left(k^{app}_{VN,NO_2}[^\bullet NO_2] + k^{app}_{VN,HOONO}[HOONO]\right)(P^0)^{-1}$, one has:

$$k'^{,n}_{VN} \cong k'^{,n}_{VN,RNS}$$

$$= \frac{[NO_2^-]}{P^0}\left\{k^{app}_{VN,NO_2}\frac{k'_{f,HO^\bullet}(1+\tau) + \left(k_{NO_2^-,^3VN^*}[^3VN^*] + k_{NO_2^-,VN^{\bullet+}}[VN^{\bullet+}]\right)}{k'_{loss,NO_2} + k_{VN,NO_2}[VN] + k_{VN^{\bullet+},NO_2}[VN^{\bullet+}]}\right.$$

$$\left. + \frac{k^{app}_{VN,HOONO}\,k'_{f,HO^\bullet}\,\tau'}{k'_{iso} + k_{VN,HOONO}[VN]}\right\} \qquad \text{(Eq.SI-14)}$$

The observed linear trend of $k'^{,n}_{VN}$ with respect to nitrite concentration in snow shown in Fig.s 3b,d (main manuscript) can be reasonably described with Eq.SI-14, although for 5 µmol L$^{-1}$ VN the direct photolysis

of the compound is not completely negligible (Table 1 of the main manuscript). Likewise, Eq.SI-14 may be representative of the decreasing trend of $k_{VN}^{',n}$ with [VN] (Fig.4 of the main manuscript), in particular if $k'_{f,HO^\bullet} (1 + \tau) \gg k_{NO_2^-,^3VN^*}[^3VN^*] + k_{NO_2^-,VN^{\bullet+}}[VN^{\bullet+}]$. Note that $k'_{f,HO^\bullet} (1 + \tau)$ represents the rate coefficient of $^\bullet NO_2$ formation by nitrite photolysis, while the term $k_{NO_2^-,^3VN^*}[^3VN^*] + k_{NO_2^-,VN^{\bullet+}}[VN^{\bullet+}]$ is the rate coefficient of $^\bullet NO_2$ production due to nitrite oxidation by $^3VN^*$ and $VN^{\bullet+}$.
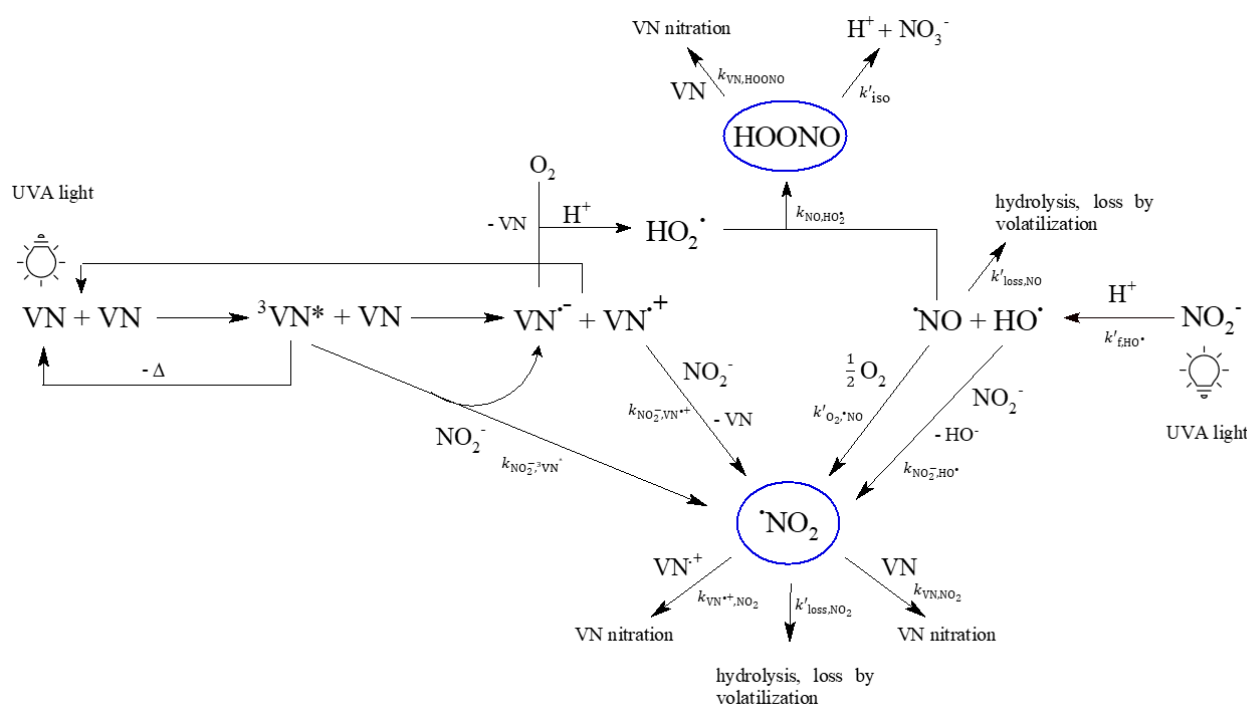


**Scheme SI-1**. Possible reactions taking place in irradiated snow samples when the main photodegradation pathway of VN is accounted for by reactions with RNS. Rate constants are reported next to the related reaction arrows.

When VN photodegradation in snow is mainly mediated by nitrite, the general form of the total photon-flux-normalized rate of VN photodegradation can be expressed as $R_{VN} = k_{VN,NO_2^-}^{app}[NO_2^-][VN](P^0)^{-1}$, where $k_{VN,NO_2^-}^{app}$ is the apparent second-order rate constant of the $NO_2^-$-mediated photodegradation of VN. At the same time, one has $R_{VN} = k_{VN}^{',n}[VN]$, where $k_{VN}^{',n}$ is the observed photodegradation rate constant.

S15

The relationship $k_{VN}^{\prime,n} = k_{VN,NO_2^-}^{app}[NO_2^-](P^0)^{-1}$ is obtained as a consequence, or alternatively $k_{VN,NO_2^-}^{app} = k_{VN}^{\prime,n} P^0([NO_2^-])^{-1}$.

$$k_{VN,NO_2^-}^{app} = \left\{ k_{VN,NO_2}^{app} \frac{k'_{f,HO^\bullet}(1+\tau) + \left(k_{NO_2^-,{}^3VN^*}[{}^3VN^*] + k_{NO_2^-,VN^{\bullet+}}[VN^{\bullet+}]\right)}{k'_{loss,NO_2} + k_{VN,NO_2}[VN] + k_{VN^{\bullet+},NO_2}[VN^{\bullet+}]} \right.$$

$$\left. + \frac{k_{VN,HOONO}^{app} \, k'_{f,HO^\bullet} \, \tau'}{k'_{iso} + k_{VN,HOONO}[VN]} \right\} \qquad \text{(Eq.SI-15)}$$

Fig.SI-8 shows the computed values of $k_{VN,NO_2^-}^{app}$ in artificial snow as a function of added sodium nitrite, when reactions with RNS are the main VN degradation pathways. Note that for 5 µmol L$^{-1}$ VN the values of $k_{VN,NO_2^-}^{app}$ are basically constant over the adopted NO$_2^-$ range, as expected from Eq.SI-15. For 50 µmol L$^{-1}$ VN, $k_{VN,NO_2^-}^{app}$ is insensitive to nitrite concentration for [NO$_2^-$] ≥ 20 µmol L$^{-1}$, while its value at [NO$_2^-$] = 5 µmol L$^{-1}$ was a little bit higher. This difference can be due to the experimental uncertainty on the measured $k_{VN}^{\prime,n}$ because of the slow photodegradation of vanillin (slightly less than 6% after 5h-long irradiation).
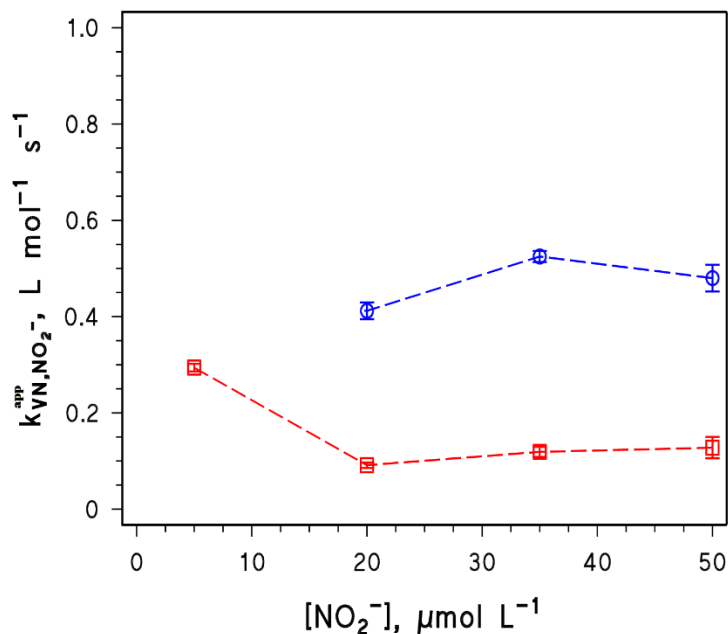
**Fig.SI-8**. Apparent second-order rate constant of VN photodegradation mediated by nitrite in artificial snow. The blue data refer to 5 µmol L$^{-1}$ as initial VN concentration, while the red ones to 50 µmol L$^{-1}$ VN.
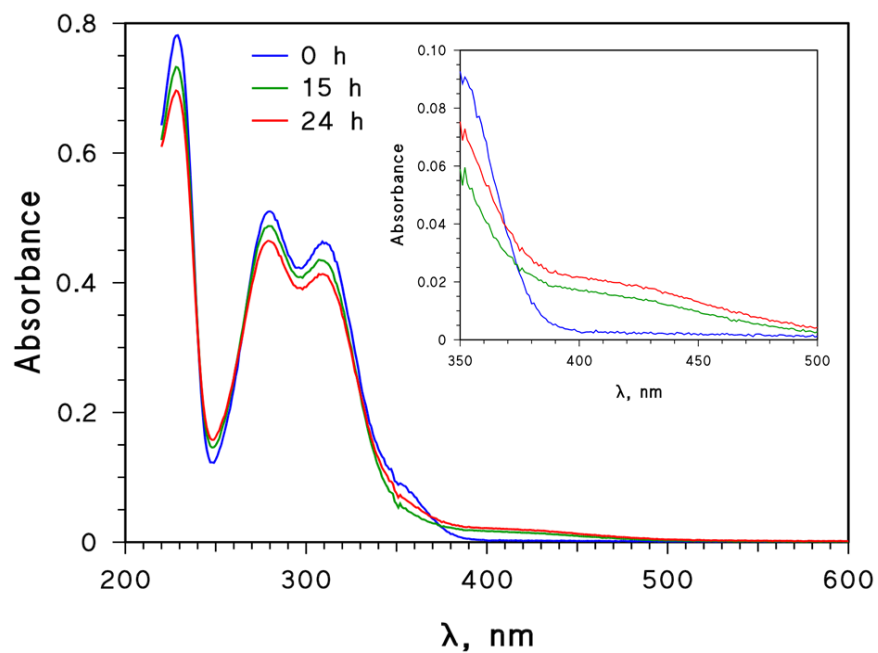


**Fig.SI-9**. Absorption spectra of (melted) artificial snow samples recorded before and after 15 - 24 h of UVA irradiation. The initial chemical composition of snow was 50 µmol L$^{-1}$ NO$_2^-$, 50 µmol L$^{-1}$ VN and 16.7 µmol L$^{-1}$ Na$_2$SO$_4$. The inset shows the increase of absorbance for $\lambda > 380$ nm after irradiation.
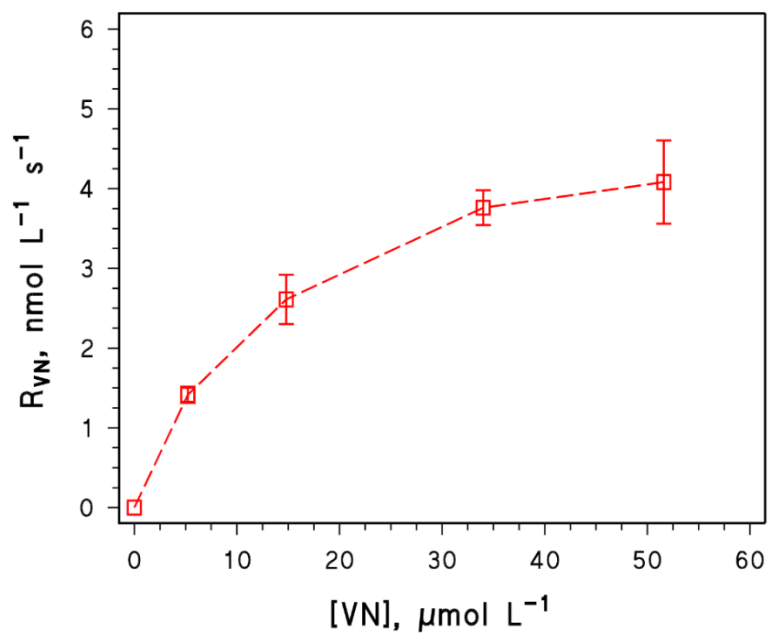
**Fig.SI-10**. Photodegradation rate of VN, as a function of initial vanillin concentration, measured in liquid water at room temperature in the presence of 50 µmol L$^{-1}$ NO$_2^-$ and Na$_2$SO$_4$ (31.6 ÷ 16.7 µmol L$^{-1}$, to fix the total solute concentration at 200 µmol L$^{-1}$).
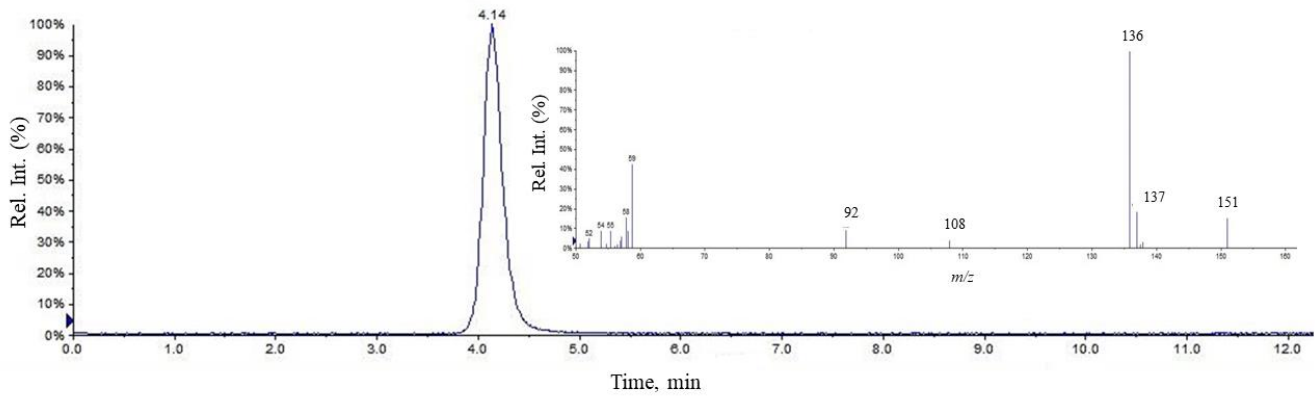
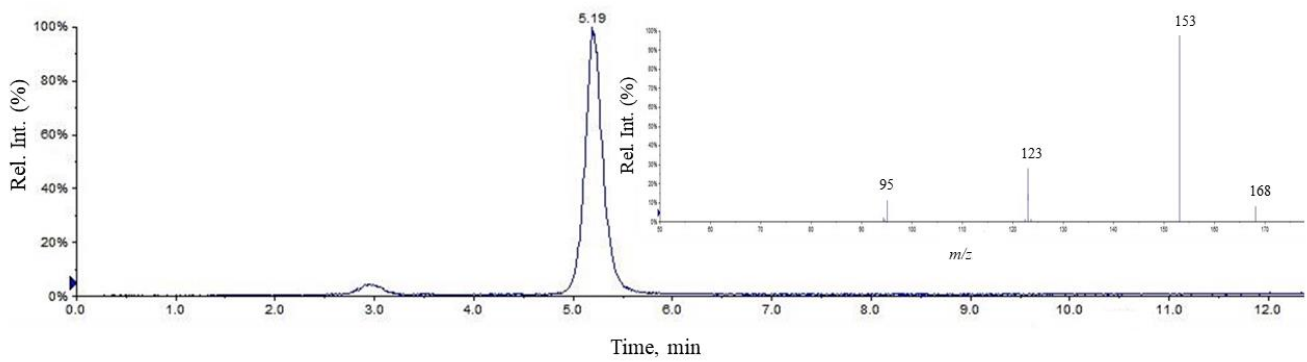**Fig. SI-11**. XIC chromatogram and related MS$^2$ spectrum of ion 151 *m/z*.



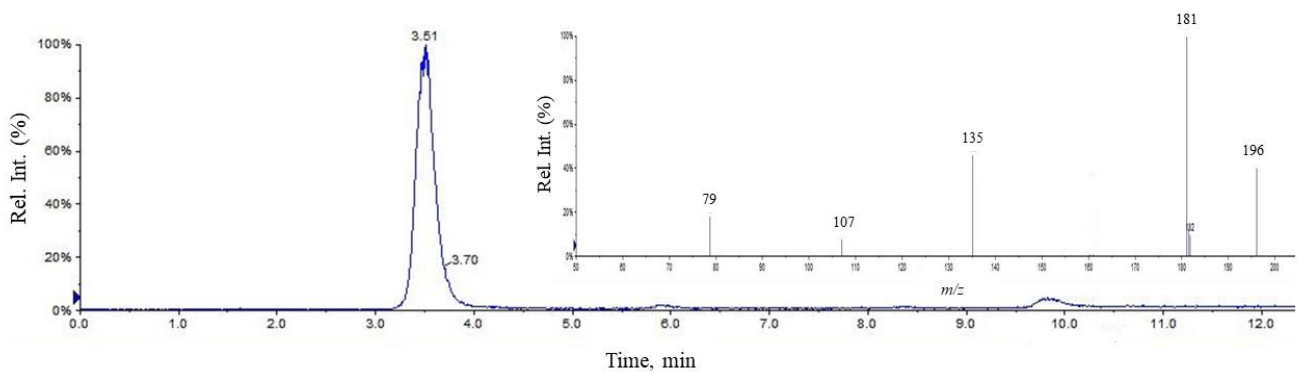**Fig. SI-12**. XIC chromatogram and related MS$^2$ spectrum of ion 168 *m/z*.



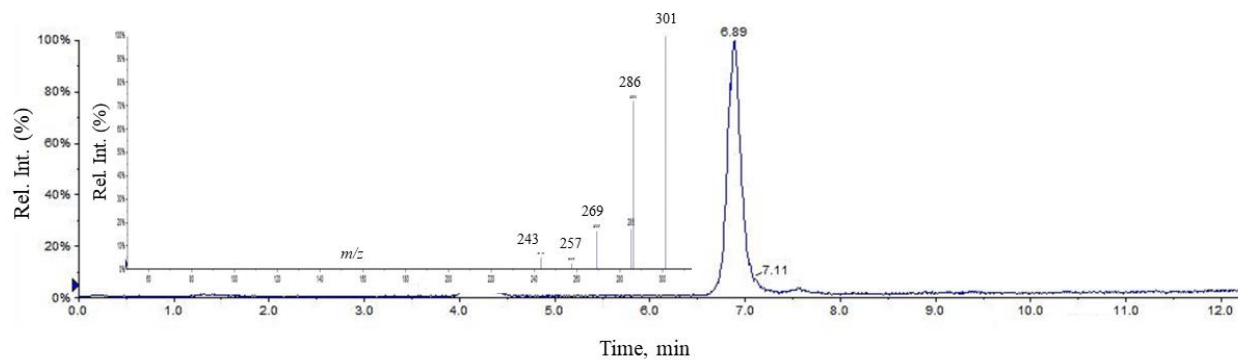**Fig. SI-13**. XIC chromatogram and related MS$^2$ spectrum of ion 196 *m/z*.

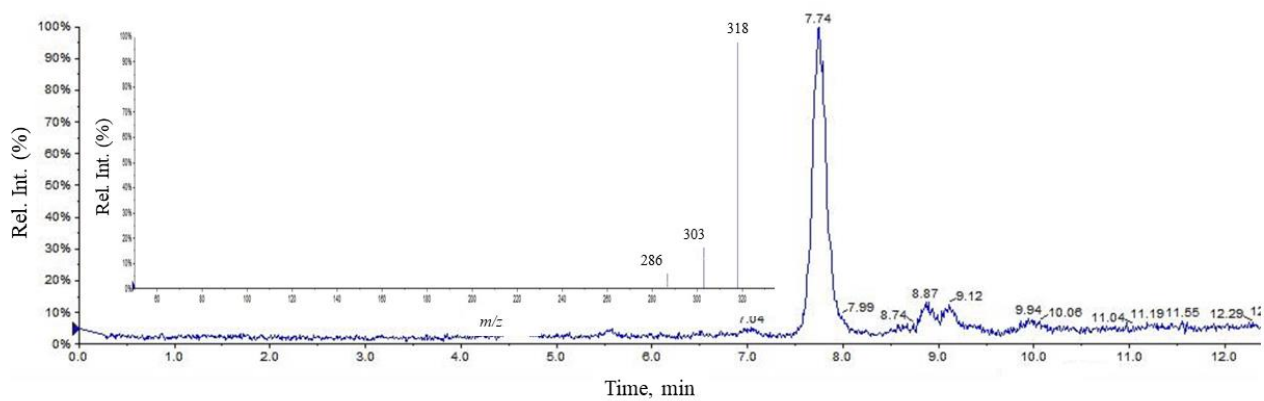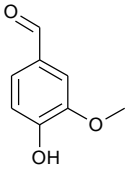**Fig. SI-14**. XIC chromatogram and related MS$^2$ spectrum of ion 301 $m/z$.



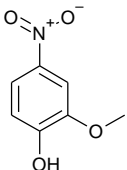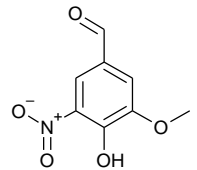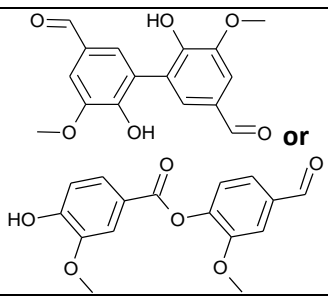**Fig. SI-15**. XIC chromatogram and related MS$^2$ spectrum of ion 318 $m/z$.

**Table SI-1**. Investigated photoproducts from VN photodegradation sensitized by nitrite. *M.M.* is the molecular mass of the compound, while $t_r$ its retention time.

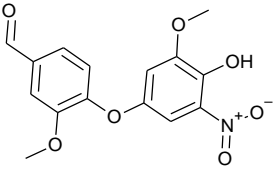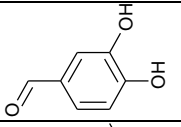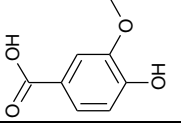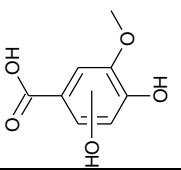| Compound (*M.M.*, g mol⁻¹) | $t_r$, min | [M-H]⁻ $m/z$ | MS² ions (abundance, proposed fragments) | Structure |
|---|---|---|---|---|
| VN (152) | 4.14 | 151 | 151 (11); 137 (35, -H-CH₂); 136 (100, -H-CH₃); 108 (10, -H-CH₃-CO); 92 (43, -H-CO-CH₃OH) |  |
| 4NG (169) | 5.19 | 168 | 168 (22); 153 (100, -H-CH₃); 123 (50, -H-CH₃-CHOH); 95 (26; -H-CH₃-CHOH-CO) |  |
| 5NVN (197) | 3.51 | 196 | 196 (62); 181 (100, -H-CH₃); 135 (44, -H-CH₃-NO₂); 107 (12, -H-CH₃-NO₂-CO); 79 (25, -H-CH₃-NO₂-2xCO) |  |
| DVN (302) | 6.89 | 301 | 301 (100); 286 (85, -H-CH₃); 269 (25, -H-CH₃OH); 257 (10, -H-CH₃-COH); 243 (13, -2xCH₃-CO) |  |
| 4NPVN (319) | 7.74 | 318 | 318 (100); 303 (24, -H-CH₃); 286 (12, -H-CH₃OH) |  |
| 3,4-dihydroxybenzaldheyde (138) | n.d.* | 137 | / |  |
| Vanillic acid (168) | n.d.* | 167 | / |  |
| Hydroxylated vanillic acid (184) | n.d.* | 183 | / |  |

*n.d. = not detected.
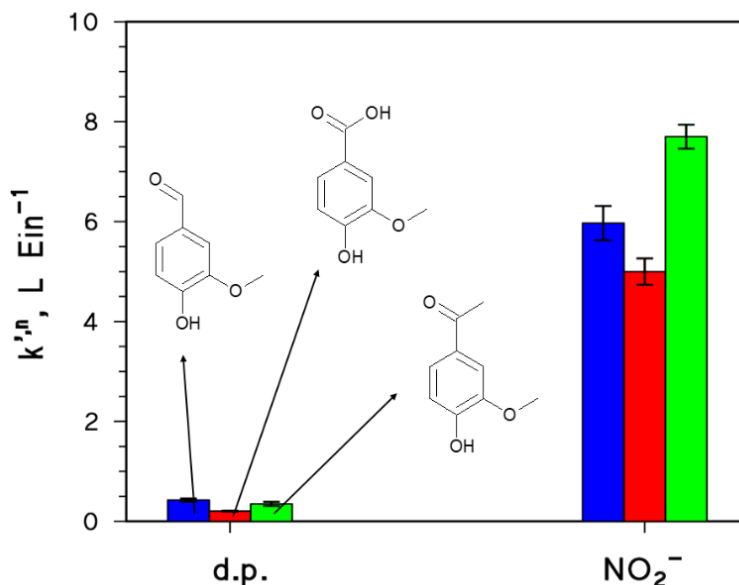
**Fig.SI-16.** Photon-flux-normalized rate coefficients of VN (blue bars), vanillic acid (red bars) and acetovanillone (green bars) by direct photolysis (*d.p.*) and in the presence of sodium nitrite (50 µmol L$^{-1}$) measured in artificial snow at 243 K. The initial concentration of the targeted compounds was 5 µmol L$^{-1}$. Snow [*TS*] was fixed at 200 µmol L$^{-1}$ by means of $Na_2SO_4$.

## References

(1)    Legagneux, L.; Cabanes, A.; Dominé, F. Measurement of the Specific Surface Area of 176 Snow Samples Using Methane Adsorption at 77 K. *J. Geophys. Res. Atmos.* **2002**, *107* (D17), ACH 5-1-ACH 5-15. https://doi.org/https://doi.org/10.1029/2001JD001016.

(2)    Domine, F.; Taillandier, A.-S.; Simpson, W. R. A Parameterization of the Specific Surface Area of Seasonal Snow for Field Use and for Models of Snowpack Evolution. *J. Geophys. Res. Earth Surf.* **2007**, *112* (F02031), 1–13. https://doi.org/10.1029/2006JF000512.

(3)    Kerbrat, M.; Pinzer, B.; Huthwelker, T.; Gäggeler, H. W.; Ammann, M.; Schneebeli, M. Measuring the Specific Surface Area of Snow with X-Ray Tomography and  Gas Adsorption: Comparison and Implications for Surface Smoothness. *Atmos. Chem. Phys.* **2008**, *8* (5), 1261–1275. https://doi.org/10.5194/acp-8-1261-2008.

(4)    Abbatt, J. P. D.; Bartels-Rausch, T.; Ullerstam, M.; Ye, T. J. Uptake of Acetone, Ethanol and Benzene to Snow and Ice: Effects of Surface Area and Temperature. *Environ. Res. Lett.* **2008**, *3* (4), 45008. https://doi.org/10.1088/1748-9326/3/4/045008.

(5)    Kieber, R. J.; Seaton, P. J. Determination of Subnanomolar Concentrations of Nitrite in Natural Waters. *Anal. Chem.* **1995**, *67* (18), 3261–3264. https://doi.org/10.1021/ac00114a024.

(6)    Li, Y. J.; Huang, D. D.; Cheung, H. Y.; Lee, A. K. Y.; Chan, C. K. Aqueous-Phase Photochemical Oxidation and Direct Photolysis of Vanillin – a Model Compound of Methoxy Phenols from Biomass Burning. *Atmos. Chem. Phys.* **2014**, *14* (6), 2871–2885. https://doi.org/10.5194/acp-14-2871-2014.

(7)    Mabato, B. R. G.; Lyu, Y.; Ji, Y.; Li, Y. J.; Huang, D. D.; Li, X.; Nah, T.; Lam, C. H.; Chan, C. K.

Aqueous Secondary Organic Aerosol Formation from the Direct Photosensitized Oxidation of Vanillin in the Absence and Presence of Ammonium Nitrate. *Atmos. Chem. Phys.* **2022**, *22* (1), 273–293. https://doi.org/10.5194/acp-22-273-2022.

(8)     Pang, H.; Zhang, Q.; Lu, X.; Li, K.; Chen, H.; Chen, J.; Yang, X.; Ma, Y.; Ma, J.; Huang, C. Nitrite-Mediated Photooxidation of Vanillin in the Atmospheric Aqueous Phase. *Environ. Sci. Technol.* **2019**, *53* (24), 14253–14263. https://doi.org/10.1021/acs.est.9b03649.

(9)     Carena, L.; Puscasu, C. G.; Comis, S.; Sarakha, M.; Vione, D. Environmental Photodegradation of Emerging Contaminants: A Re-Examination of the Importance of Triplet-Sensitised Processes, Based on the Use of 4-Carboxybenzophenone as Proxy for the Chromophoric Dissolved Organic Matter. *Chemosphere* **2019**, *237*, 124476. https://doi.org/10.1016/j.chemosphere.2019.124476.

(10)    McFall, A. S.; Anastasio, C. Photon Flux Dependence on Solute Environment in Water Ices. *Environ. Chem.* **2016**, *13* (4), 682–687. https://doi.org/doi.org/10.1071/EN15199.

(11)    Bononi, F. C.; Chen, Z.; Rocca, D.; Andreussi, O.; Hullar, T.; Anastasio, C.; Donadio, D. Bathochromic Shift in the UV–Visible Absorption Spectra of Phenols at Ice Surfaces: Insights from First-Principles Calculations. *J. Phys. Chem. A* **2020**, *124* (44), 9288–9298. https://doi.org/10.1021/acs.jpca.0c07038.

(12)    Chu, L.; Anastasio, C. Temperature and Wavelength Dependence of Nitrite Photolysis in Frozen and Aqueous Solutions. *Environ. Sci. Technol.* **2007**, *41* (10), 3626–3632. https://doi.org/10.1021/es062731q.

(13)    Buxton, G. V; Greenstock, C. L.; Helman, P. W.; Ross, A. B. Critical Review of Rate Constants for Reactions of Hydrated Electrons, Hydrogen Atoms and Hydroxyl Radicals ($\cdot$OH/$\cdot$O$^-$) in Aqueous Solution. *J. Phys. Chem. Ref. Data* **1988**, *17* (2), 513–886. https://doi.org/https://doi.org/10.1063/1.555805.

(14)    Anastasio, C.; Chu, L. Photochemistry of Nitrous Acid (HONO) and Nitrous Acidium Ion (H2ONO+) in Aqueous Solution and Ice. *Environ. Sci. Technol.* **2009**, *43* (4), 1108–1114. https://doi.org/10.1021/es802579a.

(15)    Takenaka, N.; Ueda, A.; Daimon, T.; Bandow, H.; Dohmaru, T.; Maeda, Y. Acceleration Mechanism of Chemical Reaction by Freezing:  The Reaction of Nitrous Acid with Dissolved Oxygen. *J. Phys. Chem.* **1996**, *100* (32), 13874–13884. https://doi.org/10.1021/jp9525806.